

# A Two-Sink Solution to the Self-Similar Euler Equations

Hyungjun Choi, Matei P. Coiculescu

February 18, 2026

## Abstract

We construct the first known example of a self-similar solution to the two-dimensional incompressible Euler equations whose pseudo-velocity has more than one stagnation point. The solution is also a homogeneous steady state of the Euler equations. In contrast, any homogeneous steady state with bounded vorticity necessarily admits only a single stagnation point at the origin. Our construction develops cusps in the velocity along two lines passing through the origin, thereby allowing stagnation points other than the origin.

## 1 Introduction

We consider the two-dimensional incompressible Euler equations:

$$\begin{aligned} \partial_t u + (u \cdot \nabla) u + \nabla p &= 0 \\ u(\cdot, t = 0) &= u_0(\cdot). \end{aligned} \tag{1}$$

One solves for the velocity vector field  $u(x, t)$  and scalar pressure field  $p(x, t)$  starting from initial data  $u_0(x)$ . The incompressible Euler equations in two-dimensions model the motion of inviscid fluids in thin plates. Due to a transport structure of the equations, the vorticity,  $\operatorname{curl} u$ , is transported by the velocity  $u$ , which facilitates the existence theory for weak solutions starting from quite irregular initial data (for example, the existence for  $L^1 \cap L^p$  vorticity was proven in [8]). On the other hand, uniqueness of solutions is only known when the vorticity is bounded, and non-uniqueness is only known (by convex integration arguments) due to a lack of energy conservation for  $C^{1/3^-}$  velocity. More recently, the authors of [6] used convex integration to prove non-uniqueness for  $L^{1+}$  vorticity data on  $\mathbb{T}^2$ . The question

whether unbounded and integrable ( $L^1 \cap L^p$ ) vorticity data guarantees the uniqueness of weak solutions is open and referred to as the “Yudovich Problem”.

Besides convex integration, another promising strategy for proving that there exist non-unique solutions to the Euler equations proceeds via the construction of self-similar solutions. We say that a vorticity profile  $\Omega$  is a *self-similar profile* to the incompressible Euler equations if and only if  $\Omega$  satisfies the following system of equations:

$$\begin{aligned} (\nabla^\perp \Psi - \frac{1}{\alpha} \xi) \cdot \nabla_\xi \Omega &= \Omega, \\ \Delta \Psi &= \Omega. \end{aligned} \quad (2)$$

Here we denoted  $\nabla^\perp f = (-\partial_y f, \partial_x f)$ , so the corresponding stream function profile is  $\Psi$ , the velocity profile is  $U = \nabla^\perp \Psi$ , and we have  $\operatorname{curl} U = \Omega$ . If  $\Omega$  is a self-similar profile solving Equation (2), then

$$\omega(x, t) := t^{-1} \Omega(xt^{-1/\alpha}), \quad (3)$$

is a time-dependent self-similar solution of Equation (1). The parameter  $\alpha \in (0, 2)$  determines the scaling of the solution. Let us consider polar coordinates  $(\rho, \theta)$  in the self-similar variables. Suppose that the profile  $\Omega$  has the following asymptotic behavior at  $\rho \rightarrow \infty$  (corresponding to  $|\xi| \rightarrow \infty$ ):

$$\lim_{\rho \rightarrow \infty} \frac{\Omega(\rho, \theta)}{\rho^{-\alpha}} = g(\theta),$$

where  $g(\theta)$  is a function of the polar angle only. Then we observe:

$$\lim_{t \rightarrow 0} \omega(x, t) = \lim_{t \rightarrow 0} \frac{t^{-1} \Omega(xt^{-1/\alpha}) |xt^{-1/\alpha}|^{-\alpha}}{|xt^{-1/\alpha}|^{-\alpha}} = g(\theta) |x|^{-\alpha}.$$

Therefore, any self-similar solution to the Euler equations should arise from homogeneous initial vorticity data. Moreover, the initial data should be determined by the asymptotics of the self-similar profile at infinity.

Bifurcation in the self-similar variables is believed to be a plausible non-uniqueness mechanism for the Euler equations, especially since Vishik proved the non-uniqueness of solutions with time-integrable forcing in [14] (a result further refined by the authors of [1]). We now describe the bifurcation behavior necessary for non-unique solutions to arise. If one can construct two different self-similar profiles with the same “data at infinity” in the self-similar variables, then one has proven the existence of two different self-similar solutions to the Euler equations from the same homogeneous data.

However, we remark that addressing the  $L^1 \cap L^p$  Yudovich problem using this approach requires truncating the  $(-\alpha)$ -homogeneous vorticity data away from infinity, which seems quite difficult to resolve. Indeed, overcoming this difficulty appears to require a deep understanding of the linearization of the Euler equations in the space  $L^{2/\alpha, \infty}$ . We refer the reader to [2] for further discussions on this point.

We have argued the importance of self-similar solutions to the Euler equations for the question of non-uniqueness. Homogeneous solutions to the Euler equations, like the power-law vortex  $\Omega(\xi) = |\xi|^{-\alpha}$ , are self-similar solutions to the Euler equations that are also stationary in the “physical coordinates”. Most of the qualitative properties of stationary homogeneous solutions to the two-dimensional Euler equations have been catalogued in the work [11] of Luo and Shvydkoy.

Perhaps one of the most intuitive and numerically validated mechanisms for non-uniqueness is the following bifurcation behavior: from an initial data of vorticity that is homogeneous, supported on two antipodal regions in angle, and symmetric with respect to rotation by  $\pi$ , either a single vortex spiral forms at the center of symmetry or two vortex spirals form with centers away from the center of symmetry. This bifurcation behavior was claimed to be observed numerically by the authors of [4] and discussed from the “pen and paper” point of view in [5].

The single spiral solution has been studied with mathematical rigor by several authors. Elling first proved in [9] the existence of self-similar solutions to the Euler equations from data that are small perturbations of the power-law vortex and  $m$ -fold rotationally symmetric with large  $m$ . His result was later refined by the authors of [7] and [13].

While the results in [9], [10], [13], and [7] are technically impressive, they leave the question of non-uniqueness (and even the question of how to approach this problem) completely open. In particular, the non-uniqueness scenario proposed in [4] and [5] requires the existence of a self-similar solution to the Euler equations whose pseudo-velocity has more than one stagnation point. On the other hand, all the previous constructions of self-similar spirals essentially depended on small perturbations of the inviscid power-law vortex. Consequently, all the solutions they construct have self-similar *pseudo-velocity*  $U - \frac{\xi}{\alpha}$  with a single (spiral) stagnation point.

We believe it is worthwhile for the non-uniqueness program to discover self-similar profiles with pseudo-velocity having more than one stagnation point, and this is the goal of this note. We construct the first example of such a self-similar solution to the two-dimensional incompressible Euler equations.

**Theorem.** *For any value of the scaling parameter  $\alpha \in (0, 1)$ , there exists a self-similar profile  $\Omega$  that is  $(-\alpha)$ -homogeneous and whose corresponding pseudo-velocity field  $U - \frac{\xi}{\alpha}$  has two sink stagnation points away from the origin and a saddle stagnation point at the origin.*

We call the self-similar profile we construct the *two-sink solution*. The pseudo-velocity field of the two-sink solution is pictured in Figure 1 and Figure 2. Keeping in mind the numerical experiments done in [4], we consider our two-sink solution as a plausible candidate for exhibiting the bifurcation behavior previously described. Our main theorem, in conjunction with the work showing the existence of self-similar solutions from generic data at infinity, demonstrates the feasibility of the non-uniqueness scenario proposed by Bressan and co-authors.

We note that our two-sink solution has velocity that is only Hölder continuous; however, this is not a peculiarity of our construction, but rather a consequence of the additional stagnation points. In particular, we prove in Proposition 3.7 below that any homogeneous self-similar solution to the two-dimensional incompressible Euler equations whose pseudo-velocity has more than one stagnation point has vorticity that is discontinuous along an infinite ray.

We thank Peter Constantin and Alexandru Ionescu for helpful comments on this note. We acknowledge Princeton University for its support. MPC also acknowledges the support of the National Science Foundation in the form of an NSF Graduate Research Fellowship.

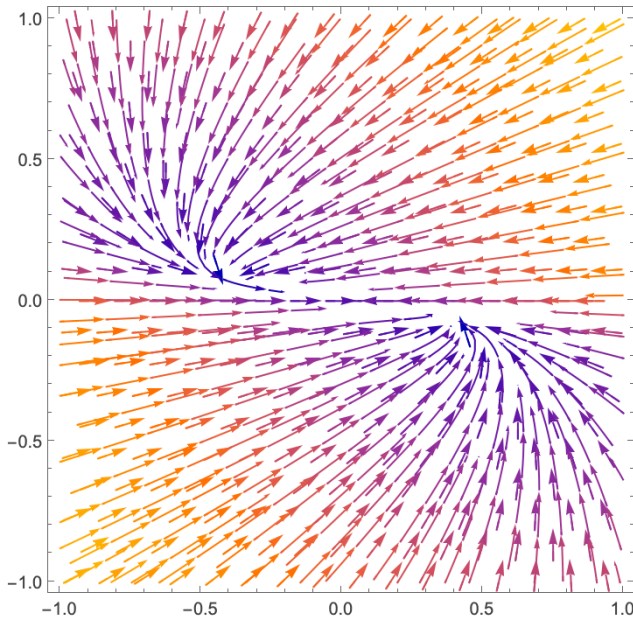


Figure 1: Vector Plot of the Pseudo-Velocity of the Two-Sink Solution when  $\alpha = \frac{3}{4}$  on  $[-1, 1]^2$

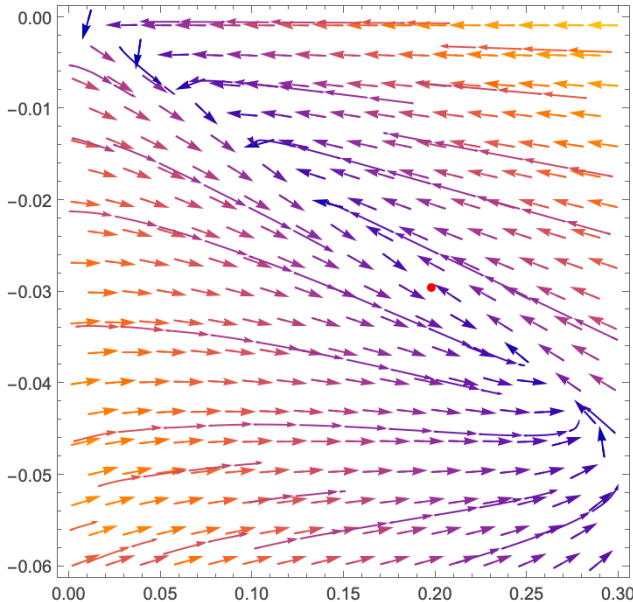


Figure 2: Vector Plot of the Pseudo-Velocity of the Two-Sink Solution when  $\alpha = \frac{3}{4}$  on  $[0, 0.3] \times [-0.06, 0]$ . The red dot is the location of a stagnation point.

## 2 Homogeneous Solutions of the Euler Equations and a Hamiltonian System

Consider a homogeneous solution  $u$  of the steady two-dimensional Euler equations. In other words, for some scalar pressure  $p$ , the vector field  $u$  satisfies the system

$$u \cdot \nabla u + \nabla p = 0$$

$$\operatorname{div} u = 0,$$

and has the form  $u = \nabla^\perp \varphi$ ,  $\varphi = r^\lambda \psi(\theta)$ , and  $p = r^{2\lambda-2} P(\theta)$ . Then,  $u = r^{\lambda-1}(-\psi' \mathbf{e}_r + \lambda \psi \mathbf{e}_\theta)$  and putting this into the steady two-dimensional Euler equations gives

$$\begin{aligned} -\lambda \psi \psi'' + (\lambda - 1)(\psi')^2 - \lambda^2 \psi^2 + 2(\lambda - 1)P &= 0, \\ P' &= 0. \end{aligned} \tag{4}$$

If  $\lambda > 0$ ,  $P$  is a constant, and  $\psi \in H^1(\mathbb{T})$  solves Equation (4), then  $u = \nabla^\perp(r^\lambda \psi(\theta)) \in L^2_{\text{loc}}$  is a steady state of the two-dimensional Euler equations. Since the solution  $(u, p)$  is homogeneous, it is also a steady solution of the two-dimensional self-similar Euler equations (Equation (2)) with self-similar variable  $\xi = x/t^{1/\alpha}$  where  $\alpha = 2 - \lambda$ . In general, we find homogeneous solutions  $\Psi = r^{2-\alpha} \psi(\theta)$  by solving the ordinary differential equation given in Equation (4), which turns out to be a Hamiltonian system.

To construct the two-sink solution, we find a homogeneous solution with pseudo-velocity vector field  $\nabla^\perp \Psi - \frac{1}{\alpha} \xi$  having two sink stagnation points. This is the first rigorous construction of solutions to the two-dimensional self-similar Euler equations whose pseudo-velocity has stagnation points other than the origin.

## 3 Construction of the Two-Sink Solution

In this section, we build upon the preliminary results on homogeneous solutions presented in the paper [11] of Luo and Shvdkoy, and we construct the two-sink solution. While Luo and Shvdkoy perform a complete classification of local solutions to the Hamiltonian system, their paper omits the construction of any particular non-trivial  $2\pi$ -periodic function  $\psi(\theta)$ . Our construction requires a fine asymptotic analysis of the period functions associated to the Hamiltonian system that will occupy us for the rest of this note.

### 3.1 Local solution

We rewrite Equation (4) as

$$\psi'' = \frac{\lambda - 1}{\lambda} \frac{(\psi')^2 + 2P}{\psi} - \lambda \psi. \quad (5)$$

If  $\psi$  is sign-definite on an interval  $I = (a, b)$  and solves Equation (5), then it is smooth in  $I$ . When a local solution is extended to its maximal interval of existence,  $\psi$  vanishes at the end points (unless an end point is  $\pm\infty$ ). If  $\psi \in C^\infty((-a, a))$  is a maximally extended local solution, then  $-\psi$  and  $\psi(-\theta)$  are also local solutions. Thus, every negative local solution is obtained by multiplying a positive solution by  $(-1)$  and vice versa. Also, every local solution is even with respect to the midpoint of the maximal interval of existence.

Equation (4), equivalently Equation (5), has a first integral that originates from the Bernoulli function  $|u|^2 + 2p$ . Since the steady two-dimensional Euler equations can be re-written as  $\omega u^\perp + \nabla(|u|^2 + 2p) = 0$ , we obtain

$$u \cdot \nabla(|u|^2 + 2p) = 0. \quad (6)$$

Assume that  $\psi$  is a positive local solution. Then, if we in addition assume the homogeneous ansatz, integrating Equation (6) yields

$$B = (2P + (\psi')^2 + \lambda^2 \psi^2) \psi^{\frac{2}{\lambda} - 2}. \quad (7)$$

Equation (5) can be rewritten using the conservation law in Equation (7):

$$\psi'' = \frac{(\lambda - 1)B}{\lambda} \psi^{1 - \frac{2}{\lambda}} - \lambda^2 \psi. \quad (8)$$

If  $(\psi, P)$  is a local solution, then  $(a\psi, a^2P)$  is also a local solution for any  $a > 0$ . Thus, we may assume  $B = 1$  or  $B = -1$  without loss of generality.

From now on, we always assume that  $1 < \lambda < 2$  (equivalently  $\alpha \in (0, 1)$ ). The streamlines of the phase portrait for the ordinary differential equation are given by the curves  $(\psi, \psi')$ , where

$$2P = B\psi^{2 - \frac{2}{\lambda}} - (\psi')^2 - \lambda^2 \psi^2$$

is always satisfied. Now we have two cases depending on the sign of  $B$ .

*Case 1.  $B = 1$*

For  $P > 0$ , the streamline is a closed smooth curve in the half plane  $\{\psi > 0\}$ , and for  $P = 0$ , the streamline touches the axis  $\{\psi = 0\}$  tangentially at the origin. For  $P < 0$ , the streamline is a smooth curve connecting  $(0, \pm\sqrt{-2P})$ .

*Case 2.  $B = -1$*

In this case, we necessarily have  $P < 0$  and that the streamline is a smooth curve connecting  $(0, \pm\sqrt{-2P})$ .

### 3.2 Gluing Local Solutions

When  $1 < \lambda < 2$  and  $P < 0$ , there are two distinct, positive, and maximal local solutions, which both connect  $(0, \pm\sqrt{-2P})$  in the phase portrait of the Hamiltonian system. Let  $\psi_+ : [0, T_+] \rightarrow \mathbb{R}_{\geq 0}$  and  $\psi_- : [0, T_-] \rightarrow \mathbb{R}_{\geq 0}$  be maximal local solutions corresponding to  $B = 1$  and  $B = -1$  respectively. Then, we can glue two solutions  $\psi_+$  and  $-\psi_-$  at the endpoint to obtain a solution  $\psi : [0, T_+ + T_-] \rightarrow \mathbb{R}$  to the original differential equation in Equation (4). From the construction,  $\psi \in C^1$  and since

$$(\psi')^2 = -2P + \text{sign}(\psi)|\psi|^{2-\frac{2}{\lambda}} - \lambda^2\psi^2, \quad (9)$$

we in fact get  $\psi \in C^{1,2-\frac{2}{\lambda}}$ .

**Remark 3.1.** *The solution in the case  $P = 0$  is a shear flow  $\psi = A|\cos(\theta)|^\lambda \in C^{1,\lambda-1}$ . Thus, a solution constructed by gluing exhibits better regularity than the shear flow solution.*

**Remark 3.2.** *It is also possible to glue in the order  $\psi_+, -\psi_+, \psi_-, -\psi_-$ .*

**Remark 3.3.** *If it happens that  $T_+ + T_- = \pi$ , then  $\psi$  is a  $\pi$ -periodic solution. Therefore, it gives a 2-fold symmetric self-similar solution to the two-dimensional Euler equations.*

Now our goal is to find values of  $(\lambda, P)$  that make  $T_+ + T_- = \pi$ . Since we have an analytic expression for the streamlines,  $T_\pm$  can be written as an integral:

$$T_\pm = \int_0^1 \frac{2}{\sqrt{\lambda^2(1-s^2) \mp x_\pm^{-2/\lambda}(1-s^{2-2/\lambda})}} ds,$$

where  $x_\pm$  are positive solutions of

$$\lambda^2 x_\pm^2 \mp x_\pm^{2-\frac{2}{\lambda}} = -2P.$$

**Theorem 3.4.** *For each  $\lambda \in (1, 2)$ , there exists a  $\pi$ -periodic solution  $(\psi, P)$  of Equation (4) obtained by gluing  $\psi_+$  and  $-\psi_-$ .*

*Proof.* For each  $\lambda \in (1, 2)$ ,  $x_{\pm}$  and  $T_{\pm}$  are functions of  $P \in (-\infty, 0)$ . As  $P \rightarrow 0^-$ , we have

$$x_+^{-\frac{2}{\lambda}}(P = 0) = \lambda^2, \quad x_-(P = 0) = 0,$$

and

$$T_+(P = 0) = \int_0^1 \frac{2}{\lambda \sqrt{s^{2-2/\lambda} - s^2}} ds = \int_0^1 \frac{2}{\sqrt{1-t^2}} dt = \pi, \quad T_-(P = 0) = 0.$$

As  $P \rightarrow -\infty$ , we have  $x_{\pm}(P = -\infty) = \infty$  and

$$T_{\pm}(P = -\infty) = \frac{2}{\lambda} \int_0^1 \frac{1}{\sqrt{1-s^2}} ds = \frac{\pi}{\lambda}.$$

Thus,  $T = T_- + T_+$  is a smooth function of  $P \in (-\infty, 0)$  such that

$$T(P = 0) = \pi, \quad T(P = -\infty) = \frac{2\pi}{\lambda} > \pi.$$

In the following section, we show that  $T$  decreases as  $-P$  increases near  $P = 0$ . Therefore, there exists  $P_* < 0$  such that  $T(P = P_*) = \pi$ .  $\square$

We can now finish the proof of Theorem 1.

**Theorem 3.5.** *For each  $\alpha \in (0, 1)$ , there exists a  $\pi$ -periodic solution  $\Psi$  of Equation (2) whose corresponding pseudo-velocity  $\nabla^{\perp}\Psi - \frac{\xi}{\alpha}$  has two sink stagnation points away from the origin and a saddle stagnation point at the origin.*

*Proof.* We have already shown in Theorem 3.4 that for every  $\lambda \in (1, 2)$ , there exists a  $\pi$ -periodic solution  $(\psi, P)$  of Equation (4). The corresponding pseudo-velocity is:

$$u - \frac{\xi}{2-\lambda} = r^{\lambda-1}(-\psi' \mathbf{e}_r + \lambda\psi \mathbf{e}_{\theta}) - \frac{r}{2-\lambda} \mathbf{e}_r.$$

At a stagnation point of the pseudo-velocity, we evidently require  $\psi = 0$  and

$$r^{\lambda-1}\psi' + \frac{r}{2-\lambda} = 0.$$

We can certainly choose some unique  $r > 0$  so that this is so. By the two fold reflection symmetry, there are exactly two stagnation points. Now, it is not difficult to see that the eigenvalues of  $\nabla u$  at the two stagnation points away from the origin are precisely  $-1$  and  $\frac{-\lambda}{2-\lambda}$ , so each of these stagnation points away from the origin is a sink. Lastly, the origin is a saddle since the flow is coming out (in) in the direction where  $\psi' < 0$  ( $> 0$ ).  $\square$

**Remark 3.6.** Suppose  $\Psi = r^\lambda \psi(\theta)$  with  $\lambda \in (1, 2)$  is a homogeneous steady state. The pseudo-velocity field  $\nabla^\perp \Psi - \frac{\xi}{\alpha}$  has a stagnation point at each angle  $\theta$  where  $\psi(\theta)$  changes sign from positive to negative. Indeed, all stagnation points except the origin are equidistant from the origin since  $|\psi'(\theta)| = \sqrt{-2P}$  whenever  $\psi(\theta) = 0$ .

We also prove the following proposition, which shows that any homogeneous self-similar solution with more than one stagnation point is necessarily irregular.

**Proposition 3.7.** Let  $\alpha \in (0, 1)$ . Suppose that  $U(\xi)$  is a homogeneous self-similar solution to the two-dimensional Euler equations. Suppose in addition that the corresponding pseudo-velocity

$$\tilde{U}(\xi) := U(\xi) - \frac{\xi}{2 - \lambda}$$

has a stagnation point in addition to the one at the origin  $\xi = 0$ . Then the vorticity  $\operatorname{curl} U$  is discontinuous on a ray from the origin.

*Proof.* We recall from Luo and Shvydkoy [11] that for  $\alpha \in (0, 1)$  (equivalently  $\lambda \in (1, 2)$ ), the only  $2\pi$ -periodic stream functions  $\psi(\theta)$  possible correspond to the power-law vortex  $\psi(\theta) = A$  for some constant  $A$ , the power-law shear flow  $\psi(\theta) = A|\cos(\theta)|^\lambda$  for some constant  $A$ , and any solution obtained by gluing two local solutions to the Hamiltonian system together.

As we observed in the proof of Theorem 3.5, if the pseudo-velocity  $\tilde{U}$  has a stagnation point for  $r > 0$ , the it necessarily occurs at an angle  $\theta$  where the stream function  $\psi(\theta) = 0$  and  $\psi'(\theta) < 0$ . It is therefore not difficult to see that both the power-law vortex and the power-law shear flow are inadmissible (for one  $\psi' = 0$  always, for the other  $\psi' = 0$  whenever  $\psi = 0$ ). The only candidates remaining are obtained by gluing. As we previously observed, any gluing of local solutions yields at most  $\psi \in C^{1,2-2/\lambda}$  regularity. In particular, the vorticity is discontinuous along the ray corresponding to the angle at which the stagnation points of  $\tilde{U}$  occur.

□

### 3.3 Asymptotics as $P \rightarrow 0^-$ of the Periods $T_\pm$

We finish the proof of Theorem 3.4 by showing that  $T = T(-P)$  decreases as  $-P$  increases near  $P = 0$ . The following uses the theory presented in [3].

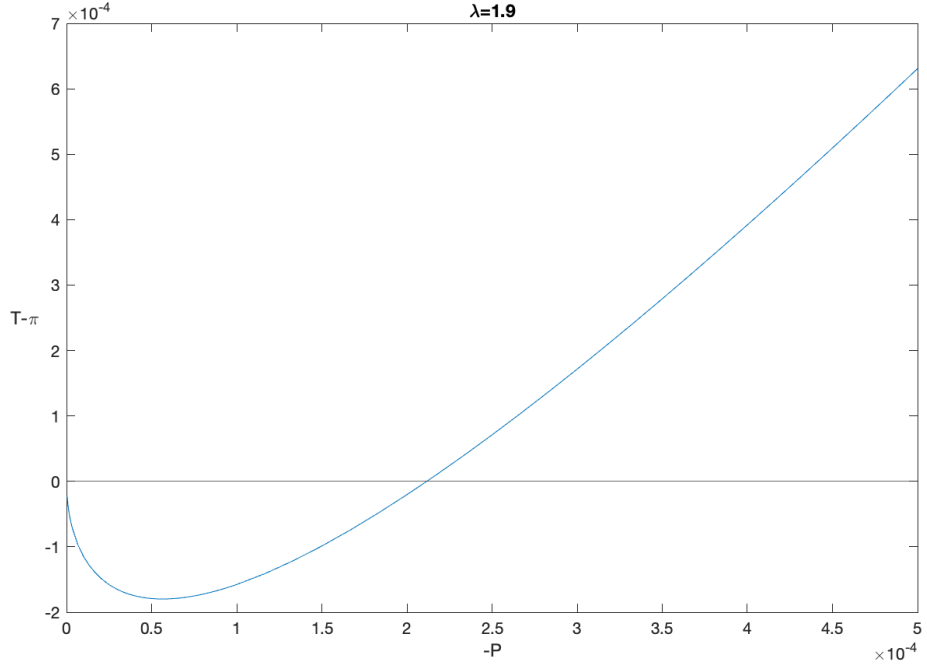


Figure 3: Graph of  $T - \pi$  near  $P = 0$  when  $\lambda = 1.9$

First, we consider  $T_+$ . Let  $a = (\lambda^2 - x_+^{-2/\lambda})/\lambda^2$ , then

$$T_+ = \frac{2}{\lambda} \int_0^1 \frac{ds}{\sqrt{s^{2-2/\lambda} - s^2 + a(1 - s^{2-2/\lambda})}}.$$

Since  $-2P\lambda^{2\lambda-2}(1-a)^\lambda = a$ ,

$$a = 2\lambda^{2\lambda-2}|P| - 4\lambda^{4\lambda-3}|P|^2 + O(|P|^3).$$

For  $\lambda \in (1, \frac{3}{2})$ , the  $a$ -derivative of the integrand is integrable, thus

$$\begin{aligned} T_+ &= \pi - \frac{2}{\lambda} \int_0^1 \frac{1 - s^{2-2/\lambda}}{(s^{2-2/\lambda} - s^2)^{3/2}} ds \cdot a + o(a) \\ &= \pi - \int_0^1 \frac{t^{\frac{1}{2}-\lambda} - t^{-\frac{1}{2}}}{(1-t)^{\frac{3}{2}}} dt \cdot a + o(a) \\ &= \pi - \frac{2\sqrt{\pi}\Gamma(\lambda)\tan(\pi\lambda)}{\Gamma(\lambda - \frac{1}{2})} \cdot a + o(a). \end{aligned}$$

Therefore, for  $\lambda \in (1, \frac{3}{2})$ ,

$$T_+ = \pi - \frac{4\lambda^{2\lambda-2}\sqrt{\pi}\Gamma(\lambda)\tan(\pi\lambda)}{\Gamma(\lambda-\frac{1}{2})}|P| + o(|P|).$$

For  $\lambda \in [\frac{3}{2}, 2)$ , let

$$f(s) = \frac{1}{\sqrt{s^{2-2/\lambda} - s^2}}, \quad g(t) = \sqrt{\frac{t}{1+t}}, \quad \phi(s) = \frac{s^{2-2/\lambda} - s^2}{1 - s^{2-2/\lambda}}.$$

Then,

$$T_+ = \frac{2}{\lambda} \int_0^1 f(s)g(a^{-1}\phi(s)) ds = \frac{2}{\lambda} \int_0^{\frac{1}{\lambda-1}} F(t)g(a^{-1}t) dt.$$

We have the following expansions for  $g, \phi$ , and  $F(t) = f(s)/\phi'(s)|_{s=\phi^{-1}(t)}$ :

$$\begin{aligned} g(t) &= 1 - \frac{1}{2}t^{-1} + \frac{3}{8}t^{-2} - \frac{5}{16}t^{-3} + \dots && \text{as } t \rightarrow \infty, \\ \phi(s) &= s^{2-\frac{2}{\lambda}}(1 + s^{2-\frac{2}{\lambda}} - s^{\frac{2}{\lambda}} + s^{4-\frac{4}{\lambda}} + \dots) && \text{as } s \rightarrow 0^+, \\ \phi^{-1}(t) &= t^{\frac{\lambda}{2\lambda-2}} \left( 1 - \frac{\lambda}{2\lambda-2}t + \frac{\lambda}{2\lambda-2}t^{\frac{1}{\lambda-1}} + \dots \right) && \text{as } t \rightarrow 0^+, \\ \frac{f(s)}{\phi'(s)} &= \frac{\lambda}{2}s^{\frac{3}{\lambda}-2} \frac{(1-s^{2-2/\lambda})^2}{\lambda-1-\lambda s^{2/\lambda}+s^2} \frac{1}{\sqrt{1-s^{2/\lambda}}} \\ &= \frac{\lambda}{2(\lambda-1)}s^{\frac{3}{\lambda}-2} \left( 1 - 2s^{2-\frac{2}{\lambda}} + \frac{3\lambda-1}{2\lambda-2}s^{\frac{2}{\lambda}} + s^{4-\frac{4}{\lambda}} + \dots \right) && \text{as } s \rightarrow 0^+, \\ F(t) &= \frac{\lambda}{2\lambda-2}t^{\frac{3-2\lambda}{2\lambda-2}} \left( 1 - \frac{2\lambda-1}{2\lambda-2}t + \dots \right) && \text{as } t \rightarrow 0^+. \end{aligned}$$

From the asymptotic expansion formula located in Appendix B, we have for  $\lambda \in (\frac{3}{2}, 2)$ ,

$$\begin{aligned} T_+ &= \frac{2}{\lambda}M[F; 1] + \frac{1}{\lambda-1}M\left[g; \frac{1}{2\lambda-2}\right]a^{\frac{1}{2\lambda-2}} - \frac{1}{\lambda}M[F; 0]a + O(a^{1+\frac{1}{2\lambda-2}}) \\ &= \pi - \frac{2\Gamma(\frac{2\lambda-1}{2\lambda-2})\Gamma(\frac{\lambda}{2\lambda-2})}{\sqrt{\pi}}a^{\frac{1}{2\lambda-2}} - \frac{\sqrt{\pi}\Gamma(\lambda)\tan(\lambda\pi)}{\Gamma(\lambda-\frac{1}{2})}a + O(a^{1+\frac{1}{2\lambda-2}}). \end{aligned}$$

Note that

$$\begin{aligned} M[F; z] &= \int_0^1 f(s)\phi(s)^{z-1} ds = \int_0^1 \frac{(s^{2-2/\lambda} - s^2)^{z-\frac{3}{2}}}{(1 - s^{2-2/\lambda})^{z-1}} ds \\ &= \frac{\lambda}{2} \int_0^1 \frac{w^{(\lambda-1)(z-1)-\frac{1}{2}}(1-w)^{z-\frac{3}{2}}}{(1 - w^{\lambda-1})^{z-1}} dw. \end{aligned}$$

Therefore, for  $\lambda \in (\frac{3}{2}, 2)$ ,

$$T_+ = \pi - \frac{2^{1+\frac{1}{2\lambda-2}} \lambda \Gamma(\frac{2\lambda-1}{2\lambda-2}) \Gamma(\frac{\lambda}{2\lambda-2})}{\sqrt{\pi}} |P|^{\frac{1}{2\lambda-2}} - \frac{2\sqrt{\pi} \lambda^{2\lambda-2} \Gamma(\lambda) \tan(\lambda\pi)}{\Gamma(\lambda - \frac{1}{2})} |P| + O(|P|^{1+\frac{1}{2\lambda-2}}).$$

For  $\lambda = \frac{3}{2}$ , we have a logarithmic singularity ( $\lambda = 3/2$  is known to be an interesting case, compare with the explicit homogeneous solutions known for this value of  $\lambda$  in [11] and the Kaden spiral in [12]):

$$T_+ = \pi - \frac{3}{4} a \log(a^{-1}) + O(a) = \pi - \frac{9}{4} |P| \log(|P|^{-1}) + O(|P|).$$

Now, we consider  $T_-$ . Let  $b = x_-^{\frac{1}{\lambda}}$ , then

$$T_- = 2b \int_0^1 \frac{ds}{\sqrt{\lambda^2 b^2 (1-s^2) + (1-s^{2-2/\lambda})}}.$$

Since  $b^{2\lambda-2} + \lambda^2 b^{2\lambda} = -2P$ ,

$$b = 2^{\frac{1}{2\lambda-2}} |P|^{\frac{1}{2\lambda-2}} - \lambda^2 2^{\frac{1}{\lambda-1}} |P|^{\frac{3}{2\lambda-2}} + o(|P|^{\frac{3}{2\lambda-2}}).$$

Therefore,

$$\begin{aligned} T_- &= 2b \int_0^1 \frac{ds}{\sqrt{1-s^{2-2/\lambda}}} + O(b^3) \\ &= \frac{2^{1+\frac{1}{2\lambda-2}} \sqrt{\pi} \lambda \Gamma(\frac{\lambda}{2\lambda-2})}{\Gamma(\frac{1}{2\lambda-2})} |P|^{\frac{1}{2\lambda-2}} + O(|P|^{\frac{3}{2\lambda-2}}). \end{aligned}$$

We conclude that

$$T = \begin{cases} \underbrace{\pi - \frac{4\lambda^{2\lambda-2} \sqrt{\pi} \Gamma(\lambda) \tan(\pi\lambda)}{\Gamma(\lambda - \frac{1}{2})}}_{< 0} |P| + o(|P|) & \text{if } \lambda \in (1, \frac{3}{2}), \\ \pi - \frac{9}{4} |P| \log(|P|^{-1}) + O(|P|) & \text{if } \lambda = \frac{3}{2}, \\ \underbrace{\pi - \frac{2^{1+\frac{1}{2\lambda-2}} \lambda \Gamma(\frac{2\lambda-1}{2\lambda-2}) \Gamma(\frac{\lambda}{2\lambda-2})}{\sqrt{\pi}} \left(1 - \sin\left(\frac{\pi}{2\lambda-2}\right)\right)}_{< 0} |P|^{\frac{1}{2\lambda-2}} + O(|P|) & \text{if } \lambda \in (\frac{3}{2}, 2). \end{cases}$$

In any cases,  $T$  is a decreasing function of  $-P$  near  $P = 0$ .

## 4 Relation to the Homogeneous Shear Flow

The asymptotic behavior of the two-sink solution as  $\lambda \rightarrow 2$  is of interest as a means of comparison with the power-law shear flow  $\Omega(x, y) = |y|^{-\alpha}$ . In particular, it appears at first sight that the two-sink approaches the power-law shear flow as  $\lambda \rightarrow 2$  (equivalently  $\alpha \rightarrow 0$ ).

Indeed, from the asymptotic expansion in the previous section we obtain

$$T = \pi - \frac{2^{1+\frac{1}{2\lambda-2}} \lambda \Gamma(\frac{2\lambda-1}{2\lambda-2}) \Gamma(\frac{\lambda}{2\lambda-2})}{\sqrt{\pi}} \left( 1 - \sin\left(\frac{\pi}{2\lambda-2}\right) \right) |P|^{\frac{1}{2\lambda-2}} + \frac{2\sqrt{\pi} \lambda^{2\lambda-2} \Gamma(\lambda) \tan((2-\lambda)\pi)}{\Gamma(\lambda - \frac{1}{2})} |P| + O(|P|^{1+\frac{1}{2\lambda-2}}).$$

So we may estimate the value of the pressure  $P^*$  at which the  $\pi$ -periodic solution is found. By using only the first three terms in the asymptotic expansion above, we have that  $P^*$  is approximately:

$$|P^*|^{\frac{2\lambda-3}{2\lambda-2}} \approx \frac{2^{\frac{1}{2\lambda-2}} \Gamma(\frac{2\lambda-1}{2\lambda-2}) \Gamma(\frac{\lambda}{2\lambda-2}) \Gamma(\lambda - \frac{1}{2})}{\pi \lambda^{2\lambda-3} \Gamma(\lambda)} \frac{1 - \cos(\frac{2-\lambda}{2\lambda-2}\pi)}{\tan((2-\lambda)\pi)}$$

This approximation for the critical pressure vanishes at  $\lambda = 2$ . Taking a series expansion in  $\lambda$  about  $\lambda = 2$ , we have the following asymptotic behavior for  $P^*$  as  $\lambda \rightarrow 2^-$ :

$$|P^*(\lambda)| \approx \frac{\pi^2}{512} (2-\lambda)^2 \approx 0.0193 \alpha^2. \quad (10)$$

These asymptotics are also verified by numerically evaluating  $T$  and finding  $P^*$ . We believe that rigorously verifying Equation (10) as  $\lambda \rightarrow 2^-$ , is an interesting problem in its own right that should be quite challenging due to a degeneracy in the asymptotic formulas as  $\lambda$  approaches 2.

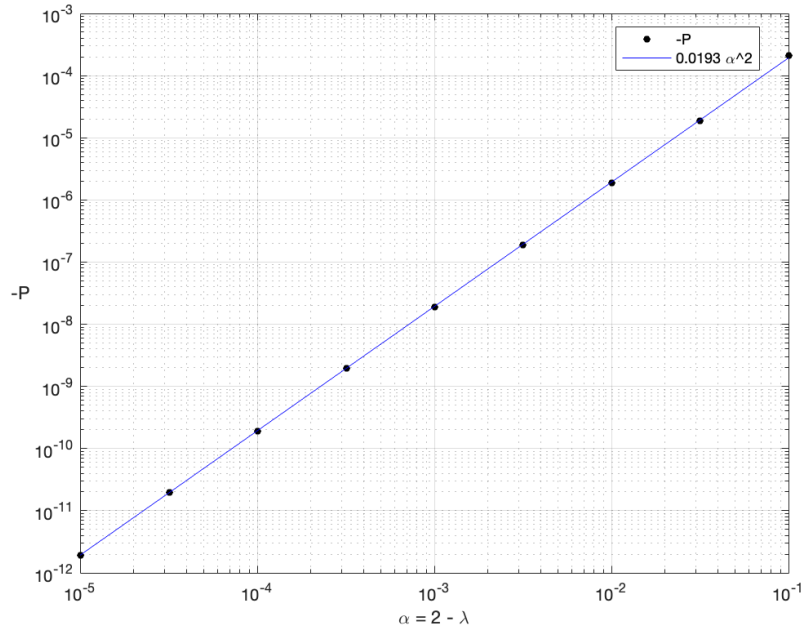


Figure 4: Log-log plot of  $P^*$  by  $\alpha$ : data for this graph are located at Appendix C.

#### 4.1 Convergence to the Shear Flow as Pressure Goes to Zero

Since this “critical pressure” value approaches zero, it seems as if the two-sink solution should approach the power-law shear flow, which has identically zero pressure, as  $\lambda \rightarrow 2$ .

To that end, we prove the following proposition, which shows convergence of the two-sink solution to the power-law shear flow at the velocity level when the critical pressure approaches zero.

**Proposition 4.1.** *Let  $\psi_P$  be a positive solution to the ordinary differential equation in Equation (9) with pressure  $P < 0$  on the interval  $[0, T_+(P)]$  corresponding to the stream function of a two-sink solution. Let  $\psi_S(x) = \lambda^{-\lambda} \sin^\lambda(x)$  be the explicit shear flow solution to Equation (9) on the interval  $[0, \pi]$  (with zero pressure). Then we have*

$$\lim_{P \rightarrow 0^-} \psi_P = \psi_S$$

*in  $C^{1,1-1/\lambda}$  on any compact subset of  $[0, \pi]$ .*

*Proof.* In this proof, we fix some  $\lambda \in (1, 2)$ . In particular, when we say that a constant depends “only” on something else, we exclude from consideration the dependence on  $\lambda$ .

We recall that the positive function  $\psi_P$  satisfies Equation (9):

$$(\psi'_P)^2 = -2P + \psi_P^{2-\frac{2}{\lambda}} - \lambda^2 \psi_P^2.$$

By the standard theory of ordinary differential equations,  $\psi_P$  is smooth on  $(0, T_+(P))$  and vanishes at the endpoints of the interval.

Suppose first that there exists a sequence  $P_n \rightarrow 0^-$  such that the solutions  $\psi_n := \psi_{P_n}$  satisfy  $\|\psi_n\|_{L^\infty} \rightarrow \infty$  as  $n \rightarrow \infty$ . Since  $1 < \lambda < 2$  we know  $2 - 2/\lambda < 2$ . Therefore, if  $x_n$  is the number in the interval  $[0, T_+(P_n)]$  at which the  $L^\infty$  bound for each  $\psi_n$  is saturated and if  $\psi_n(x_n) := A_n$ , we have

$$0 \leq (\psi'_n)^2 = -2P_n + A_n^{2-2/\lambda} - \lambda^2 A_n^2 < 0,$$

if we take  $n$  large enough. This is a contradiction, so we may conclude that

$$A := \sup_{-1 < P < 0} \|\psi_P\|_{L^\infty} < \infty,$$

or equivalently that the solutions  $\psi_P$  are uniformly bounded in  $P$  near zero. Since  $1 < \lambda < 2$ , we know  $2 - 2/\lambda > 0$ , so we immediately conclude that

$$\sup_{-1 < P < 0} \|\psi_P\|_{Lip} < L(A),$$

where  $L(A)$  is a constant depending only on  $A$ . Equivalently, the family of functions  $\psi_P$  have Lipschitz constant uniform in  $P$  near zero.

However, if  $\psi_P$  is Lipschitz, then  $-2P + \psi_P^{2-\frac{2}{\lambda}} - \lambda^2 \psi_P^2$  is  $C^{0,2-2/\lambda}$  Hölder regular, with Hölder norm depending only on  $L(A)$ , the uniform Lipschitz bound of  $\psi_P$ .

In addition,  $\pm \sqrt{-2P + \psi_P^{2-\frac{2}{\lambda}} - \lambda^2 \psi_P^2}$  is  $C^{0,1-1/\lambda}$  Hölder regular, with Hölder norm depending only on  $L(A)$ , the uniform Lipschitz bound of  $\psi_P$ . We conclude that  $\psi_P \in C^{1,1-1/\lambda}$ , with Hölder norm depending solely on  $A$ , the uniform bound in  $P$  on  $\|\psi_P\|_{L^\infty}$ .

By (a straightforward modification of) the Arzelà-Ascoli theorem, we conclude that there exists a sequence  $P_m \rightarrow 0^-$  such that  $\psi_m := \psi_{P_m}$  converges in  $C^{1,1-1/\lambda}$  to some  $C^{1,1-1/\lambda}$  function  $\psi_\infty$  on any compact subset of  $[0, \pi]$ . By the uniform boundedness, the limit is unique, in the sense that taking any sequence  $P \rightarrow 0^-$  makes  $\psi_P$  converge to  $\psi_\infty$ . We also remark that since  $\psi_P \geq 0$  for each  $P$ , we certainly have  $\psi_\infty \geq 0$  on  $[0, \pi]$ . It remains to show that  $\psi_\infty = \psi_S$ .

By the convergence proven earlier, we know

$$(\psi'_\infty)^2 = \psi_\infty^{2-\frac{2}{\lambda}} - \lambda^2 \psi_\infty^2.$$

Since  $\psi_\infty \geq 0$ , we may assume that  $\psi_\infty = f^\lambda$  for some function  $f \geq 0$ . The ordinary differential equation satisfied by  $f$  is precisely

$$(f')^2 + f^2 = \lambda^{-2},$$

so it is clear that  $f(x) = \lambda^{-1} \sin(\lambda x)$ . We conclude that  $\psi_\infty = \psi_S$ .  $\square$

**Remark 4.2.** *As noted earlier, the two-sink solution is more regular than the power-law shear flow, in a way that precludes analogous uniform convergence of the two-sink to the shear flow at the vorticity level.*

## Appendix

### A The Mellin Transform and its Analytic Continuation

Suppose  $f : [0, \infty) \rightarrow \mathbb{C}$  is a function that for some  $\alpha < \beta$ ,

$$f(t) = O(t^{-\alpha}) \text{ as } t \rightarrow 0, \quad f(t) = O(t^{-\beta}) \text{ as } t \rightarrow \infty.$$

Then, the Mellin transform  $M[f; z]$  is defined on a strip  $\alpha < \operatorname{Re} z < \beta$  as

$$M[f; z] = \int_0^\infty t^{z-1} f(t) dt.$$

The Mellin transform  $M[f; z]$  is a holomorphic function of  $z$  on the strip  $\alpha < \operatorname{Re} z < \beta$ . The inverse Mellin transform is given by

$$f(t) = \frac{1}{2\pi i} \int_{c-i\infty}^{c+i\infty} t^{-z} M[f; z] dz, \quad \alpha < c < \beta.$$

From this, it is possible to deduce the Parseval-Plancherel identity for the Mellin transform:

$$\int_0^\infty f(t)g(t) dt = \frac{1}{2\pi i} \int_{c-i\infty}^{c+i\infty} M[f; z]M[g; 1-z] dz.$$

Suppose  $f(t) = \sum_{k=0}^\infty c_k t^{a_k}$  as  $t \rightarrow 0^+$ . Then, the Mellin transform  $M[f; z]$  can be extended to a meromorphic function on a left half plane  $\operatorname{Re} z < \beta$  with

simple poles at  $z = -a_k$  for  $k = 1, 2, \dots$ , and  $\text{res}_{z=-a_k} M[f; z] = c_k$ . Let  $f(t) = \sum_{k=0}^{N-1} c_k t^{a_k} 1_{[0,1)}(t) + f_N(t)$ . Then, on the strip  $\alpha < \text{Re } z < \beta$ , we get

$$M[f; z] = \sum_{k=0}^{N-1} c_k \int_0^1 t^{z+a_k-1} dt + M[f_N; z] = \sum_{k=0}^{N-1} \frac{c_k}{z+a_k} + M[f_N; z].$$

The expression above is a meromorphic function on a strip  $-a_N < \text{Re } z < \beta$  with simple poles at  $z = -a_0, \dots, -a_{N-1}$ .

Similarly, if  $f(t) = \sum_{k=0}^{\infty} d_k t^{-b_k}$  as  $t \rightarrow \infty$ . Then, the Mellin transform  $M[f; z]$  can be extended to a meromorphic function on a right half plane  $\text{Re } z > \alpha$  with simple poles at  $z = b_k$  for  $k = 1, 2, \dots$ , and  $\text{res}_{z=b_k} M[f; z] = -d_k$ .

## B Asymptotic Expansions for Integrals

Consider

$$I(\lambda) = \int_0^L f(t)g(\lambda t) dt$$

as  $\lambda \rightarrow \infty$ . From the Parseval-Plancherel identity for Mellin transform, we get

$$\int_0^L f(t)g(\lambda t) dt = \frac{1}{2\pi i} \int_{c-i\infty}^{c+i\infty} \lambda^{-z} M[f; 1-z] M[g; z] dz.$$

Suppose

$$f(t) = \sum_{k=0}^{\infty} c_k t^{a_k} \text{ as } t \rightarrow 0^+, \quad g(t) = \sum_{l=0}^{\infty} d_l t^{-b_l} \text{ as } t \rightarrow \infty.$$

If there is no  $a_k$  and  $b_l$  such that  $a_k + 1 = b_l$ , then simple poles of  $M[f; 1-z]$  and  $M[g; z]$  does not overlap. By shifting the contour to right, we pick up residues and the following asymptotic expansion is obtained:

$$I(\lambda) = \sum_{k=0}^{\infty} c_k M[g; a_k + 1] \lambda^{-a_k-1} + \sum_{l=0}^{\infty} d_l M[f; -b_l + 1] \lambda^{-b_l}.$$

If  $a_k + 1 = b_l = \gamma$  for some  $k, l$ , then  $M[f; 1-z] M[g, z]$  has a double pole at  $z = -\gamma - 1$ . In this case, the corresponding term in the asymptotic expansion becomes

$$c_k d_l \lambda^{-\gamma} \log \lambda - \left( \text{res}_{z=-\gamma-1} M[f; 1-z] M[g, z] \right) \lambda^{-\gamma}.$$

Now, consider

$$J(\lambda) = \int_0^L f(s)g(\lambda \phi(s)) ds$$

where  $\phi : [0, L] \rightarrow [0, M]$  be strictly increasing bijection. Then, substituting  $t = \phi(s)$  gives

$$J(\lambda) = \int_0^M \underbrace{\frac{f(s)}{\phi'(s)}}_{=F(t)} g(\lambda t) dt.$$

An asymptotic expansion can be obtained by the computation above, while

$$M[F; z] = \int_0^M t^{z-1} f(s) \frac{dt}{\phi'(s)} = \int_0^L \phi^{z-1}(s) f(s) ds.$$

## C Numerical Data

$\lambda$	$-2P^*$	$\alpha^{-2}P^*$
1.9	$4.2333434 \cdot 10^{-4}$	0.0212
1.96838	$3.7657484 \cdot 10^{-5}$	0.0188
1.99	$3.7510429 \cdot 10^{-6}$	0.0188
1.99684	$3.7903849 \cdot 10^{-7}$	0.0190
1.999	$3.8277711 \cdot 10^{-8}$	0.0191
1.99968	$3.9359471 \cdot 10^{-9}$	0.0192
1.9999	$3.8507873 \cdot 10^{-10}$	0.0193
1.999968	$3.9461 \cdot 10^{-11}$	0.0193
1.99999	$3.8547 \cdot 10^{-12}$	0.0193

Figure 5: Numerical investigation of  $P^*$  for several values of  $\lambda$  approaching 2

Mathematica code for the generation of the vector plots in Figure 1 and Figure 2 and Matlab code for the computation of the data above and the generation of Figure 3 and Figure 4 may be found at the website of the second named author.

<https://web.math.princeton.edu/~mc3498/>.

## References

- [1] Albritton, D., Brué, E., Colombo, M., De Lellis, C., Giri, V., Janisch, M., Kwon, H. *Instability and non-uniqueness for the 2D Euler equations, after M. Vishik.* Annals of Mathematics Studies, 219. (2024).
- [2] Binz, T., Coiculescu, M.P. *Stability of the Inviscid Power-Law Vortex.* arXiv:2411.13397
- [3] Bleistein, N., Handelsman, R.A. *Asymptotic expansions of integrals.* 2nd ed., Dover Publications, Inc., New York, 1986. xvi+425 pp.
- [4] Bressan, A., Shen, W. *A posteriori error estimates for self-similar solutions to the Euler equations.* Disc. Cont. Dyn. Sys. Vol. 41. No. 1. pp. 113-130. (2021).
- [5] Bressan, A., Murray, R. *On self-similar solutions to the incompressible Euler equations.* J. Diff. Equations. Vol. 269. pp. 5142-5203. (2020).
- [6] Bruè, E., Colombo, M., Kumar, A., *Flexibility of Two-Dimensional Euler Flows with Integrable Vorticity.* to appear in Duke Math. J., arXiv:2408.07934
- [7] Choi, H. *Asymmetric Self-similar Spiral Solutions of two-dimensional Incompressible Euler Equations.* arXiv:2507.05059
- [8] DiPerna, R. J., Majda, A. J., *Oscillations and concentrations in weak solutions of the incompressible fluid equations.* Comm. Math. Phys. Vol. 108. pp. 667–689. (1987).
- [9] Elling, V. *Algebraic spiral solutions of 2d incompressible Euler.* J. Diff. Equations. Vol 255. No 11. pp. 3749-3787. (2013).
- [10] Elling, V. *Self-Similar 2d Euler Solutions with Mixed-Sign Vorticity.* Comm. Math. Phys. Vol 348. pp. 27–68. (2016).
- [11] Luo, K., Shvydkoy, R. *2D Homogeneous Solutions to the Euler Equations.* Comm. PDE. Vol. 40. pp.1666-1687. (2015).
- [12] Kaden, H. *Aufwicklung einer unstabilen Unstetigkeitsfläche.* Ingenieur-Archiv, 2:140–168, (1931).
- [13] Shao, F., Wei, D., Zhang, Z. *Self-Similar Algebraic Spiral Solution of two-dimensional Incompressible Euler Equations.* Ann. PDE. Vol. 11. (2025).
- [14] Vishik, M., *Instability and non-uniqueness in the Cauchy problem for the Euler equations of an ideal incompressible fluid. Part I and II.* arXiv:1805.09426, arXiv:1805.09440